International Journal of Computational Materials
Science and Engineering
Vol. 8, No. 3 (2019) 1950009 (21 pages)

DOI: 10.1142/S204768411950009X

Stochastic mixed mode stress intensity factor of center cracks FGM plates using XFEM

Achchhe Lal* and Kanif Markad†
Mechanical Engineering Department
SVNIT, Surat, Gujarat 395007, India
**achchhelal@med.svnit.ac.in; lalachchhe@yahoo.co.in*
†*kmarkad13@gmail.com*

Received 8 November 2018
Revised 21 June 2019
Accepted 22 June 2019
Published 6 August 2019

Extended finite element method (XFEM) and second-order perturbation technique (SOPT) were combinedly utilized using interaction integral (M-integral) through partition of unity method to find out the mean and variance of mixed mode stress intensity factor (MMSIF). Uncertain system parameters are considered in material properties, crack length, crack orientation, gradient coefficients in the present study. MMSIF in a numerical example with center crack is computed to validate the accuracy of the presented model. Finally, typical numerical results are presented to examine the different modulus ratios, crack angle, crack length, position of crack and tensile, shear and combined loadings with uncertain system properties on the MMSIF.

Keywords: XFEM; center crack; FGM plate; SOPT; COV; MMSIF.

1. Introduction

Functionally graded materials (FGMs) are one type of composite materials in which different types of constituent phases vary in one or more directions to achieve targeted performance with better reliability during applications. Due to the presence of constituent phases, this type of material structures provides better strength and toughness with desired structural integrity. Compared with classical and conventional composites, FGMs hold many superior thermal, mechanical, wear-resistant and corrosion-resistant properties [Suresh and Mortensen, 1998]. This is the reason behind the increasing interest of researchers in FGMs in recent years. During manufacturing and processing of FGM structures, some form of discontinuity always appears in the form of imperfections. These imperfections may be cracks, holes, voids, inclusions, porosities and so on. Crack may be considered as one of the

*Corresponding author.

imperfections. The presence of crack in a structure reduces strength and toughness of structures considerably and even more reduction in toughness under the action of combined loadings acting simultaneously or individually in the form of tensile, shear and combination of both loadings. Under this condition, it is essential to examine the toughness behavior in terms of mixed mode stress intensity factor (MMSIF) under applied loadings for optimum performance. Analysis of fracture behavior using conventional FEM poses certain difficulties to update the mesh during evolving crack and cumbersome. To relieve this difficulty, Asadpoure *et al.* [2006], Asadpoure and Mohammad [2007] and Mohammadi [2008] proposed the extended finite element method (XFEM) to model the cracks without remeshing by introducing discontinuous enrichment functions by application of XFEM for fracture behavior of composite and FGM structures.

The study related to statistics of fracture analysis of cracked FGMs or conventional structures using conventional and extended FEM approach is limited due to complexity involved for solving random governing equation. In this direction, Lin and Yang [1983] established a new statistical theory based on linear regression for the analysis of fatigue crack propagation depending on the concept of fracture mechanics and diffusive Marcov random processes. Besterfield *et al.* [1991] evaluated the probability of fatigue failure and fatigue crack growth using probabilistic finite element method in the presence of uncertainties in component geometry, applied loads, material properties and crack geometries. Liu *et al.* [1996] evaluated a curvilinear fatigue growth problem using first-order reliability method (FORM) based on total derivative method, second-order reliability method (SORM) based on Lagrange multiplier formulation and Monte-Carlo simulation. Lal and Palekar [2016, 2017] evaluated the stochastic mixed mode SIF of laminated composite plate with arbitrary cracks by assuming random material properties, crack length, crack angles and lamination angle using XFEM combined with SOPT and MCS. Nouy *et al.* [2007, 2008], Nouy and Clément [2010] proposed a stochastic-based analysis of random multi-phase materials using spectral finite element method in the framework of XFEM based on partition of unity method.

The FGMs structure with crack requires more attention due to involvement of various levels of randomness, particularly material properties and fracture parameter in terms of crack length and crack angles. For efficient and reliable design, effect of these random variables should be quantified accurately; otherwise, predicted response differs from actual response and structure may fail or fracture after some time. For proper handling of randomness at each stage of design parameters, specialized probabilistic tools based on perturbation method and computer-based MCS are being widely used so far. Lal *et al.* [2017] evaluated the MMSIF and their crack growth analysis with influence of input random variables of laminated composite beam uniaxial, uniform tensile, shear and combined stresses using XFEM based on partition of unity approach using SOPT and MCS. Lal *et al.* [2018] evaluated the MMSIF and their crack growth analysis with influence of input random variables of

laminated composite beam uniaxial, uniform tensile, shear and combined stresses using XFEM based on partition of unity approach using SOPT and MCS. Lang *et al.* [2013] evaluated heat transfer phenomena in composite materials with uncertain material interface using XFEM based on level set method in conjunction with polynomial chaos. Lal *et al.* [2017] predicted the normalized mean and variance of MMSIF and reliability analysis of a central cracked laminated composite plate subjected to uniaxial tension. They examined the effect of input assumed random system parameters with crack parameters, lamination angle and loading parameters in terms of mean, standard deviation and probability density function (PDF) and safety factor of cracked laminated composite plate. Khatri and Lal [2017, 2018] evaluated MMSIF and crack growth analysis of isotropic plate subjected to tensile, shear and combined loadings with circular hole using XFEM. They examined the effect of crack parameters and radius of hole of statistics of MMSIF with input random parameters.

Chen *et al.* [2001] proposed a new method for shape sensitivity analysis of first mode SIF for a crack in a homogeneous, isotropic and nonlinearly elastic body subject to tensile loading conditions based on the continuum sensitivities and first-order reliability method. Rahman and Chen [2005] again developed similar method for shape sensitivity analysis of first mode SIF for a crack in a homogeneous, isotropic, and nonlinearly elastic body based on the continuum sensitivities and first-order reliability method through J integral and direct differentiation. Rahman [1995, 2000] proposed a probabilistic model for nonlinear fracture-mechanics analysis through-walled-cracked pipes subject to bending loads for estimating energy release rates, J-tearing and structural reliability. Rahman [2006] proposed a new dimensional decomposition method to obtain probabilistic characteristics of crack driving forces and reliability analysis of cracked structures subjected to random load, material properties and crack geometry using MCS. Xu and Rahman [2004, 2005] developed a new decomposition multivariate dimension-reduction computational method for predicting failure probability of structural and mechanical systems subject to random loads, material properties and geometry using Taylor series expansion method and direct MCS. Chakraborty and Rahman [2008, 2009] presented a new moment-modified polynomial dimensional decomposition (PDD) method for stochastic multiscale fracture analysis of three-dimensional, particle-matrix, functionally graded materials (FGMs) subject to arbitrary boundary conditions with various discontinuities using MCS. Rahman and Rao [2001, 2002] developed a stochastic element-free Galerkin method for reliability analysis of linear-elastic structures with spatially varying random material properties using first-order reliability method through mesh-free method.

Reddy and Rao [2008] evaluated probabilistic fracture response and reliability analysis of the linear-elastic cracked structures subjected to mixed-mode loading conditions using stochastic-based fractal finite element method (FFEM) using FORM and MCS. Tomar and Zhou [2005] presented the deterministic and stochastic

analysis of dynamic fracture in heterogeneous microstructures of an Al2O3/TiB ceramic composite system to quantify the random material properties and fracture parameters using perturbation method. Evangelatos and Spanos [2011] examined the probabilistic crack propagation direction using Neumann expansion method based on MCS through peridynamic-based stochastic fracture mechanics.

Guo and Noda [2007] developed the piecewise exponential (PE) model for the investigation of crack in FGMs with arbitrary properties. By (PE) model, the crack vertical to the free surfaces was studied. The theory of residues, singular integral equation and integral transform methods was applied. The nonhomogeneous properties of samples and relative SIFs were analyzed and the validity of the PE model is shown. Guo and Noda [2008] utilized the inplane impact loading conditions to analyze the dynamic response of FGMs for a crack crossing the interface. The problem is reduced to the singular integral equation in the Laplace transform domain by using Fourier integral transforms, singular integral equation method and Laplace transforms. The peak and static values and overshoot characteristics of the dynamic stress intensity factors are analyzed. Shrivastava and Lal [2013] evaluated stress state at the zone of a crack tip by a predictive method to know component life, which depends on the stress intensity factor. Here, they used finite element approach to predict the SIFs in a finite plate with multiple edge cracks. Jamia *et al.* [2016] utilized mixed mode crack (MM crack) into the infinite graded medium where the crack is arbitrarily oriented with material gradient. The exponential variation of material properties and normal and tangential tractions applied on crack surfaces are related to further applied load. The effects of the material gradient nonhomogeneity parameter, lattice parameter, crack length, crack angular orientation were studied for the nonlocal stress field near the crack tip. Lal and Kapania [2013] evaluated the second-order statistics of critical stress intensity factor of single edge-notched fiber-reinforced composite plate with random material properties using C0 finite element method in conjunction with first-order perturbation technique via iso-parametric quarter point element through displacement correlation method.

Despite excellent characteristics, structure made of FGMs suffers from a number of shortcomings, mainly in the form of unstable crack formation which can be initiated and propagated under different production imperfections and service circumstances. Therefore, the study of the crack stability and load bearing capacity of these types of structures, which directly affect the safety and economics of many important industries, has become one of the important topics of research for the computational mechanic's community.

A limited analysis is available on the fracture analysis of FGM structures with random system properties. However, the fracture response of the FGMs panels with random system parameters using XFEM with random system properties is rarely dealt by researchers to the best of author's knowledge. As a matter of fact, these issues, which are at base of the problem, provided the motivation for the present study.

2. Formulation

Consider a center cracked body with domain denoted by Ω and outer boundary Γ containing a crack, denoted by Γ_c, as shown in Fig. 1. The body is subjected to uniform body/volume forces b, and the traction forces are applied at the boundary Γ_t. The displacement boundary conditions are applied at the boundary surface, Γ_u, where $\Gamma = \Gamma_u \cup \Gamma_t \cup \Gamma_c$. The parameters $\bar{u}$ and $\bar{t}$ are prescribed displacement and tractions, respectively. The crack surface Γ_c is assumed to be traction-free.

2.1. *Governing equation*

The equilibrium equations and boundary conditions for a body B can be written as [Mohammadi, 2008; Belytschko and Black, 1999]:

$$\nabla \cdot \sigma + f^q = 0 \quad \text{in } \Omega; \quad \sigma \cdot n = f^t \quad \text{on } \Gamma_t; \quad u = \bar{u} \quad \text{on } \Gamma_u; \quad \sigma \cdot n = 0 \quad \text{on } \Gamma_c, \tag{1}$$

where σ is the Cauchy stress tensor and $\mathbf{n}$ is the unit outward normal vector, $\bar{u}$ and $\bar{t}$ are prescribed displacement and tractions, respectively. The parameters f^q and f^t are the body force and external traction **vectors**, respectively. The cracks faces considered are traction-free.

The displacement of any point x located within the cracked domain, with modeling a crack, crack surfaces and crack tips in the XFEM, can be written as [Asadpoure

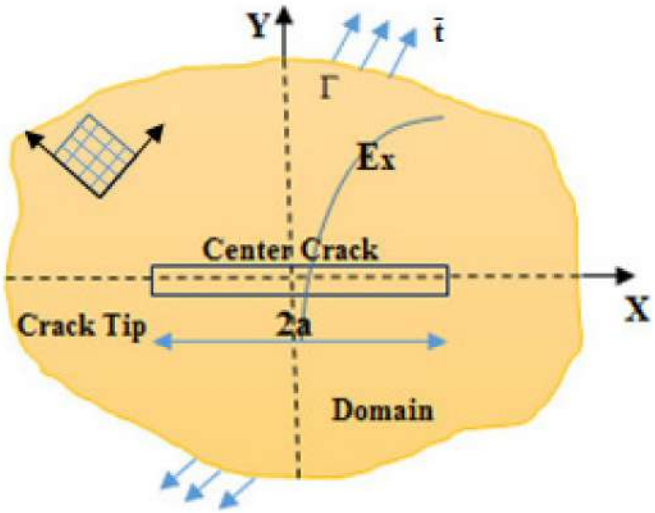

Fig. 1. An arbitrary FGM body with central crack, subjected to traction and displacement $\bar{u}$, having global Cartesian coordinate (X,Y).

et al., 2006; Belytschko and Black, 1999]:

$$u^h(x) = \sum_{j=1}^{n} L_j(x)u_j + \sum_{k=1}^{crf} L_k(x)(H(\xi(x)) - H(\xi(x_k)))a_k + \sum_{l=1}^{ct_1} L_l(x)\left(\sum_{t=1}^{ct_1 f}(F_t^1(x) - F_t^1(x_l))b_l^{t_1}\right) + \sum_{m=1}^{ct_2} L_m(x)\left(\sum_{t=1}^{ct_2 f}(F_t^2(x) - F_t^2(x_m))b_m^{t_2}\right), \quad (2)$$

where the *crf* are the set of nodes that have the crack face but not the crack tip in their support domain, *ct*1 and *ct*2 are the sets of nodes associated with crack tips 1 and 2 in their influential domain, respectively. *uj* are the nodal displacements (standard degrees of freedom), *ak*, $b_l^{t_1}, b_m^{t_2}$ are the **vectors** of additional degrees of freedom for the nodes located on crack face and the two crack tips, respectively. The parameters F_t^1, F_t^2 represent the crack tip enrichment functions for both the crack tips.

The function $H(\xi(x))$ used in Eq. (2) is the Heaviside function and the value is $+1$ if the point is on the positive side of the crack face and -1 otherwise, represented as

$$H(\xi) = \begin{cases} +1 & \xi \in \Omega^+ \\ -1 & \xi \in \Omega^-. \end{cases} \quad (3)$$

Nodes that belong to $ct1f$ and $ct2f$ are enriched with the crack-tip enrichment functions $F_t^1(x)$, $F_t^2(x)$, respectively. The nodes which contain the crack within their support domain and do not belong to $ct1f$ or $ct2f$ are enriched with the Heaviside function $H(\xi)$.

In the present problem, linear elastic fracture problem is considered. The kinematic equation for plane stress condition can be written as [Asadpoure *et al.*, 2006; Asadpoure and Mohammad, 2007; Mohammadi, 2008]:

$$\varepsilon_{ij} = C_{ij}\sigma_j. \quad (4)$$

For isotropic and orthotropic materials with three mutually perpendicular orthogonal planes of elastic symmetry, the strain (C_{ij}) can be written as:

$$C_{ij} = \begin{bmatrix} C_{11} & C_{12} & C_{16} \\ C_{21} & C_{22} & C_{26} \\ C_{16} & C_{26} & C_{66} \end{bmatrix} = \begin{bmatrix} \frac{1}{E} & -\frac{\nu}{E} & 0 \\ -\frac{\nu}{E} & \frac{1}{E} & 0 \\ 0 & 0 & \frac{1}{G} \end{bmatrix}, \quad (5)$$

where E and υ are the Young's modulus and Poisson's ratio for isotropic material, respectively. For orthotropic materials, E and υ can be further defined as [Asadpoure

et al., 2006; Asadpoure and Mohammad, 2007; Mohammadi, 2008]:

$$E = \sqrt{E_{11}E_{22}}, \quad \nu_{12} = \nu_{21} \quad \text{and} \quad G = G_{12}, \tag{6}$$

where E_{11} and E_{22} are Young's moduli of elasticity along longitudinal and transverse directions, G_{11} and υ_{12} are the shear modulus and Poisson's ratio along the longitudinal direction, respectively.

The cracked system of a linear equation in global form can be written as [Asadpoure *et al.*, 2006; Asadpoure and Mohammad, 2007; Mohammadi, 2008]:

$$[K]\{\mathbf{u}^h\} = \{\mathbf{F}\}, \tag{7}$$

where $[K]$ is the stiffness matrix, $\{\mathbf{u}^h\}$ is the displacement vector of degrees of freedom for nodes (for both classical FEM and enriched obtained by XFEM) and $\{\mathbf{F}\}$ is the external force vector. The global matrix $[K]$ and force **vectors** $\{\mathbf{F}\}$ are calculated by assembling matrices and **vectors** for each element as given below [Asadpoure *et al.*, 2006; Asadpoure and Mohammad, 2007; Mohammadi, 2008].

The crack tip enrichment functions fi(r, θ) which include all possible displacement states can be given as [Asadpoure *et al.*, 2006; Asadpoure and Mohammad, 2007; Mohammadi, 2008; Lin and Yang, 1983]:

$$F_l(r,\theta) = \sqrt{r}\left[\cos\frac{\theta_1}{2}\sqrt{g_1(\theta)}, \cos\frac{\theta_2}{2}\sqrt{g_2(\theta)}, \sin\frac{\theta_1}{2}\sqrt{g_1(\theta)}, \sin\frac{\theta_2}{2}\sqrt{g_2(\theta)}\right]. \tag{8}$$

For orthotropic material, the variable $gj(\theta)$ can be written as:

$$g_j(\theta) = [1 + (-1)^j l^2 \sin^2\theta_j]^{\frac{1}{2}}; \quad l^2 = (\gamma_1^2 + \gamma_2^2) \quad \text{with } j = 1, 2, \tag{9}$$

where

$$\gamma_1^2 = \frac{1}{2}(\sqrt{a_2} + a_1) \quad \gamma_2^2 = \frac{1}{2}(\sqrt{a_2} - a_1) \tag{10}$$

in which

$$\theta_j = \arctan\left(\frac{\gamma_2 l^2 \sin\theta}{\cos\theta + (-1)^j l^2 \gamma_1 \sin\theta}\right) \quad \text{with } a_1 = \frac{(\alpha_1 + \alpha_2 - 4\beta_1\beta_2)}{2}, a_2 = \alpha_1\alpha_2. \tag{11}$$

The parameters $\alpha_1, \alpha_2, \beta_1$ and β_2 are defined as [Mohammadi, 2008]:

$$\alpha_1 = \frac{c_{66}}{c_{11}}, \quad \alpha_2 = \frac{c_{66}}{c_{11}}, \quad \beta_1 = \frac{c_{12} + c_{66}}{2c_{11}}, \quad \beta_2 = \frac{c_{12} + c_{66}}{2c_{66}}, \tag{12}$$

where c_{ij} $(i, j = 1, 2, 6)$ are elements of compliance matrix as defined in Eq. (5).

2.2. *Formulation of MMSIFs*

For the calculation of MMSIF of the homogeneous orthotropic material, the M-integral method based on superimposition of auxiliary and actual fields is incorporated in the present approach.

The J integral can be obtained by superposition of the actual and auxiliary states of J integrals by assuming M interaction integral as:

$$J = J^{\text{act}} + J^{\text{aux}} + M, \tag{13}$$

where J^{act} and J^{aux} are the actual and auxiliary states of J integrals, respectively [Asadpoure *et al.*, 2006; Asadpoure and Mohammad, 2007; Mohammadi, 2008].

From Eq. (13), the M integral can be expressed as [Kleiber and Hien, 1992]:

$$M = \int_A \left[\sigma_{ij}\frac{\partial u_i^{\text{aux}}}{\partial x} + \sigma_{ij}^{\text{aux}}\frac{\partial u_i}{\partial x} - W_{st}^m \Delta_{1J}\right]\frac{\partial q}{\partial x_j}dA. \tag{14}$$

For linear elastic conditions

$$W_{st}^m = \frac{1}{2}(\sigma_{ij}\varepsilon_{ij}^{\text{aux}} + \sigma_{ij}^{\text{aux}}\varepsilon_{ij}). \tag{15}$$

The strain of the auxiliary field must be chosen by the strain–stress relationship so as to satisfy the equilibrium as well as traction-free condition. After some manipulations, the following equation is obtained to evaluate the M integral and expressed as [Asadpoure *et al.*, 2006; Asadpoure and Mohammad, 2007; Mohammadi, 2008]:

$$M = 2m_{11}K_{\text{I}}K_{\text{I}}^{\text{aux}} + m_{12}(K_{\text{I}}K_{\text{II}}^{\text{aux}} + K_{\text{I}}^{\text{aux}}K_{\text{II}}) + 2m_{22}K_{\text{II}}K_{\text{II}}^{\text{aux}}, \tag{16}$$

where

$$\begin{aligned} m_{11} &= -\frac{C_{22}}{2}\text{Im}\left(\frac{\mu_1+\mu_2}{\mu_1\mu_2}\right), \\ m_{12} &= -\frac{C_{22}}{2}\text{Im}\left(\frac{1}{\mu_1\mu_2}\right) + \frac{C_{11}}{2}\text{Im}\,(\mu_1\mu_2) \quad \text{and} \\ m_{22} &= -\frac{C_{11}}{2}\text{Im}(\mu_1+\mu_2), \end{aligned} \tag{17}$$

where μ_1 and μ_2 are the roots of quadratic equation.

The stress intensity factor can then be obtained by considering the two states such as M(I) and M(II) and solving a system of linear algebraic equations. These two states can be written as M(I): ($K_{\text{I}}^{\text{aux}} = 1$, $K_{\text{II}}^{\text{aux}} = 0$) and M(II): ($K_{\text{II}}^{\text{aux}} = 1$, $K_{\text{I}}^{\text{aux}} = 0$).

The MMSIF in terms of first and second mode SIF (*KI* and *KII*) associated with auxiliary and actual states can be evaluated by calculating M by using Eq. (16) with solving a system of linear algebraic equations as [Asadpoure *et al.*, 2006; Asadpoure and Mohammad, 2007; Mohammadi, 2008]:

$$M^{(\text{I})} = 2m_{11}K_{\text{I}} + m_{12} \quad \text{and} \quad M^{(\text{II})} = m_{12}K_{\text{I}} + 2m_{22}K_{\text{II}}. \tag{18}$$

2.3. *Crack growth analysis*

In crack propagation analysis, maximum circumferential stress criteria for linear elastic fracture mechanics are used. This criterion is based on the evaluation of mixed-mode stress intensity factors. According to this criterion, it is assumed that

(1) the crack initiation will occur when the maximum hoop stress reaches a critical value, and (2) the crack will grow in a direction θc in which circumferential stress $\sigma_{\theta\theta}$ is the maximum. The direction is obtained by determining the MMSIF using the domain form of interaction integral around the crack tip by assuming that the crack surfaces are traction-free. The circumferential stress in the direction of crack propagation is a principal stress. Hence, the crack propagation direction is determined by taking the shear stress equal to zero and can be expressed as:

$$\sigma_{r\theta} = \frac{1}{\sqrt{2\pi r}} \cos\left(\frac{\theta}{2}\right)\left(\frac{1}{2}K_{\mathrm{I}} \sin\theta + \frac{1}{2}K_{\mathrm{II}}\left(3\cos\theta - 1\right)\right) = 0. \tag{19}$$

This leads to the equation for the crack propagation direction θcr in local crack tip coordinate system, written as:

$$\theta_{cr} = 2\arctan\left(\frac{1}{4}\right)\left(\frac{K_{\mathrm{I}}}{K_{\mathrm{II}}} + \sqrt{\frac{K_{\mathrm{I}}}{K_{\mathrm{II}}} + 8}\right) = 0. \tag{20}$$

According to this criterion, maximum propagation angle θ_{cr} is limited to 70.5° for pure mode II cracks. The criterion basically works well for traction-free crack surfaces.

2.4. *Stochastic analysis using perturbation method*

Consider a class of problems in which the zero mean random variables are small when compared with their mean parts. We use Taylor series expansion and neglect the third and higher order terms since second order approximation is sufficient to quantify structural response uncertainties with required accuracy in the case of most sensitive applications.

The static and random part of the stress intensity factor K is a function of static and random parts of MMSIF for mode-I KI and mode-II KII, respectively, and can be shown as [Lal *et al.*, 2017, 2018]:

$$K = f(K_n) \quad \text{where } n = \begin{cases} \mathrm{I} & \text{for mode I} \\ \mathrm{II} & \text{for mode II.} \end{cases} \tag{21}$$

The value of K_n depends on different random variables (bi) which are correlated or uncorrelated on each other with mean μ_{b_i} and standard deviation σ_{b_i}; the MMSIF can be further written as:

$$\text{if } n = \mathrm{I} \quad \text{then } K_{\mathrm{I}} = K_{\mathrm{I}}(b_1, b_2, b_3, \ldots, b_n) \tag{22}$$

$$\text{and if } n = \mathrm{II} \quad \text{then } K_{\mathrm{II}} = K_{\mathrm{II}}(b_1, b_2, b_3, \ldots, b_n). \tag{23}$$

The mean values of K_{I} or K_{II} after introducing random variables can be obtained by expanding using Taylor series up to second order about their mean values

$\mu_{b_1}, \mu_{b_2}, \ldots, \mu_{b_n}$ [Kleiber and Hien, 1992; Kaminski, 2002]:

$$K = K_{\mathrm{I}}(\mu_{b_1}, \mu_{b_2}, \ldots, \mu_{b_n}) + \sum_{i=1}^{n}(x_i - \mu_{b_i})\frac{\partial K_{\mathrm{I}}}{\partial a_i} + \frac{1}{2}\sum_{i=1}^{n}\sum_{j=1}^{n}(x_i - \mu_{b_i})(x_j - \mu_{bj})\frac{\partial^2 K_{\mathrm{I}}}{\partial b_i b_j}. \tag{24}$$

The mean of first and second order SIF, K_{I} and K_{II}, is denoted by E (K') and can be expressed as:

$$E(K'_{\mathrm{I}}) \approx K_{\mathrm{I}}(\mu_{b1}, \mu_{ab}, \ldots, \mu_{b_i}) \quad \text{and} \quad E(K'_{\mathrm{II}}) \approx K_{\mathrm{II}}(\mu_{b1}, \mu_{b2}, \ldots, \mu_{bi}). \tag{25}$$

Similarly, the first and second order variance of K_{I} and K_{II} can be expressed as

$$\begin{aligned} \mathrm{Var}(K_{\mathrm{I}}) &= \sum_{i=1}^{n}\sum_{j=1}^{n}\frac{\partial K_{\mathrm{I}}}{\partial b_i}\frac{\partial K_{\mathrm{I}}}{\partial b_j}\mathrm{cov}(b_i, b_j) \quad \text{and} \\ \mathrm{Var}(K_{\mathrm{II}}) &= \sum_{i=1}^{n}\sum_{j=1}^{n}\frac{\partial K_{\mathrm{II}}}{\partial b_i}\frac{\partial K_{\mathrm{II}}}{\partial b_j}\mathrm{cov}(b_i, b_j), \end{aligned} \tag{26}$$

where n is the total number of random variables and cov(bi, bj) is the covariance of bi and bj. The covariance matrix of correlated random variables can be further written as [Fleming *et al.*, 1997; Hadlar and Sollerc, 1998]:

$$\mathrm{cov}\,(b_i, b_j) = [C]\,[C'], \tag{27}$$

where

$$[C] = \begin{bmatrix} \sigma_{b_1}^2 & \mathrm{cov}(b_1, b_2) & \cdots & \mathrm{cov}(b_1, b_i) \\ \mathrm{cov}(b_2, b_1) & \sigma_{b_2}^2 & \cdots & \mathrm{cov}(b_2, b_i) \\ \cdots & \cdots & \cdots & \cdots \\ \mathrm{cov}(b_i, b_1) & \mathrm{cov}(b_i, b_2) & \cdots & \sigma_{b_i}^2 \end{bmatrix} \quad \text{and}$$

$$[C'] = \begin{bmatrix} 1 & \rho_{b_1,b_2} & \cdots & \rho_{b_1,b_i} \\ \rho_{b_2,b_1} & 1 & \cdots & \rho_{b_2,b_i} \\ \cdots & \cdots & \cdots & \cdots \\ \rho_{b_i,b_1} & \rho_{b_i,b_2} & \cdots & 1 \end{bmatrix}, \tag{28}$$

where

$$\begin{aligned} \sigma_{b_1}, \sigma_{b_2}, \ldots, \sigma_{b_i} &= \mathrm{cov}(b_1, b_2, \ldots, b_i) \times K_r(\mu_{b_1}, \mu_{b_2}, \ldots, \mu_{b_i}) \quad \text{and} \\ \rho_{b_i,b_j} &= \frac{\mathrm{cov}(b_i, b_j)}{b_i \cdot b_j}. \end{aligned} \tag{29}$$

Here cov(bi, bj) and ρ_{b_i,b_i} are the covariance between random variables and correlation coefficient (COC) and coefficient of variance (COV) among the different input random variables, respectively.

For statistically independent (uncorrelated) random variables, the value of COC is assumed as zero whereas for correlated random variables, COC can be assumed as any value.

In the second order mean using SOPT, the mean of first and second order SIF, K_{I} and K_{II}, can be written as [Hadlar and Mahadavan, 2000]:

$$E(K_{\mathrm{I}}'') = K_{\mathrm{I}}(\mu_{b_1}, \mu_{b_2}, \ldots, \mu_{b_n}) + \frac{1}{2}\mathrm{var}\{K_{\mathrm{I}}\} \quad \text{and}$$
$$E(K_{\mathrm{II}}'') = K_{\mathrm{II}}(\mu_{b_1}, \mu_{b_2}, \ldots, \mu_{b_n}) + \frac{1}{2}\mathrm{var}\{K_{\mathrm{II}}\}. \tag{30}$$

The corresponding second variance matrix of first and second order SIF, K_{I} and K_{II}, will be the same as given in Eq. (26).

It is to be noted that to estimate the second order variance, the information on the third and fourth order moments of the bi must be available. However, in most cases, this information is not available. Therefore, the use of second order mean and the first order variance are considered adequate for most practical engineering applications. The standard deviation (SD) may be obtained by square root of variance. The coefficient of variance (COV) of MMSIF is obtained by the ratio of standard deviation to mean of the MMSIF.

The first order variance, Eq. (26), the derivative of response variables w.r.t. input random variables (bi), i.e., $(\partial K_r/\partial b_i)$ using FOPT, is difficult to evaluate due to complex expression and derivation. So, the derivative of response variables can be obtained using central difference method of finite difference analysis (FDA).

The first order derivatives calculated using FDA can be written as:

$$\frac{\partial K_r}{\partial b_i} = \frac{K_r(b_i + \delta b_i) - K_r(b_i - \delta b_i)}{2\delta b_i}, \tag{31}$$

where δbi is a perturbation of the design parameter, i.e., the coefficient of variation (COV) of random system parameters from their mean values. The expected mean and SD are evaluated by mean centered SOPT and by employing an MCS.

3. Results and Discussion

The uniaxial tensile, shear and combined loadings are applied in perpendicular direction to crack propagation (unless otherwise stated). The interaction integral is calculated within the domain of size rd $= 3\sqrt{a}$. Here a is the effective length from the crack tip. For the computation of the results, total 30×60 elements are considered in the analysis.

Using the computer programme code in MATLAB, MMSIF in terms of mean and COV for the center crack composite plate under uniaxial tensile, shear and combined loadings is evaluated. XFEM and SOPT are used to find out the normalized mean and COV of MMSIF. Applying the random system parameters in crack length, crack orientation, gradient coefficients, uniaxial tensile loading and its effect are examined.

The basic system random variables (bi) used in this paper for center cracks composite laminated plates are defined as:

$$b_1 = E_{11}, \quad b_2 = E_{22}, \quad b_3 = v_{12}, \quad b_4 = a, \quad b_5 = \theta,$$
$$b_6 = G_{12}, \quad b_7 = \alpha, \quad b_8 = \beta, \quad b_9 = \gamma,$$

where E_{11}, E_{22}, a, α are the longitudinal, transverse Young's modulus, crack length and crack angle, respectively.

The normalized first and second mode SIFs ($K_{\mathrm{I}}, K_{\mathrm{II}}$) used here for the combined loadings (tensile and shear) in the present analysis are represented as:

$$K_{\mathrm{I}} = \bar{K}_{\mathrm{I}}/\sigma\sqrt{\pi a} \quad \text{and} \quad K_{11} = \bar{K}_{\mathrm{II}}/\sigma\sqrt{\pi a}, \quad \text{for tensile stress;}$$
$$K_{\mathrm{I}} = \bar{K}_{\mathrm{I}}/\tau\sqrt{\pi a} \quad \text{and} \quad K_{11} = \bar{K}_{\mathrm{II}}/\tau\sqrt{\pi a}, \quad \text{for shear stress;}$$
$$K_{\mathrm{I}} = \bar{K}_{\mathrm{I}}/\zeta\sqrt{\pi a} \quad \text{and} \quad K_{11} = \bar{K}_{\mathrm{II}}/\zeta\sqrt{\pi a}, \quad \text{for combined stress.}$$

The parameters L and W are the total length and width of the plate, respectively. The Young's modulus written in terms of the exponential function is given as:

$$E(x) = E_1 e^{\beta x}, \quad 0 \le x \le W,$$

where gradient coefficient β can be written as

$$\beta = \log(E_1/E_2).$$

Before, proceeding over use of FGM material, it is necessary to understand SIF variation between isotropic material and FGM material. Table 1 shows the comparison of SIF in isotropic and FGM ($\beta = 0.1$) plate with respect to crack length. It is observed that under the action of tensile loading, first mode SIF variation in isotropic plate is larger than that in FGM plate by 1.12%, 0.07%, 1.31% and 4.4%, respectively. Similarly, second mode SIF is 17%, 15%, 14.2% and 18.3% larger in isotropic plate than in FGM plate. The result clearly revealed that with the use of FGM material resistance to crack propagation and arresting the crack, values of K_{I} and K_{II} get reduced in FGM than isotropic material. This is the main reason to study the FGM plate under the action of various loading conditions, and we also

Table 1. Comparison of SIF in isotropic and FGM ($\beta = 0.1$) plate with respect to crack length.

Crack length (a)	SIF	Isotropic plate	FGM plate
0.1	K_{I}	1.2019	1.1884
	K_{II}	0.0028	0.0023
0.15	K_{I}	1.2840	1.2831
	K_{II}	0.0096	0.0081
0.2	K_{I}	1.3580	1.3402
	K_{II}	0.0218	0.0187
0.25	K_{I}	1.4946	1.4287
	K_{II}	0.0398	0.0325

observe the effect of randomness in different parameters for the better stability and performance of the structure or mechanical component under operation.

The geometry of FGM plate considering center crack subjected to uniaxial tensile, shear and combined loadings with crack enrichment in the form of crack face and crack tip is shown in Figs. 2(a) and 2(b). Figure 2(c) shows the stress distribution in the FGMs plate subjected to tensile loading and Fig. 2(d) for the shear loading, respectively. It is observed from the figures that whenever the loading is applied over the specimen or structure contains the cracks, there will be change in the stress distribution contour from the cracked region. Under tensile loading condition, the gathering of stresses will be in the upper part, while in case of shear, that will be in left part of the crack.

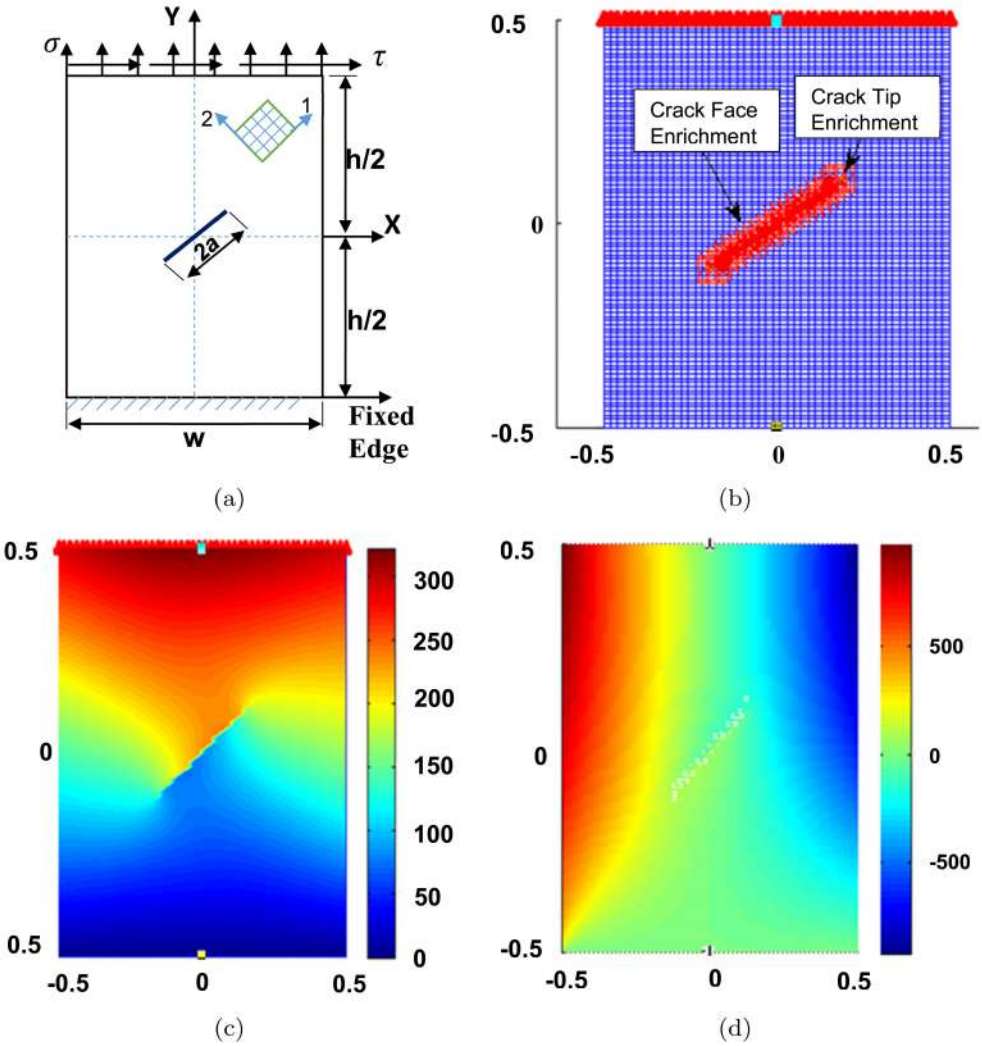

Fig. 2. Geometry of FGM plate with (a) single centre cracks subjected to uniaxial loading, (b) crack enrichments, (c) stress contour for tensile loading and (d) stress contour for shear loading.

Table 2. Normalized SIF for edge cracked plate under membrane loading for different values of α, β, γ.

α, β, γ	Present model	Mohammadi [2008]	Guo and Noda [2007]
	K_{I}	K_{I}	K_{I}
(0, 0, 0)	1.12	1.003	0.9969
(0.1, 0.1, 0.1)	1.18	1.0762	1.075
(0.25, 0.25, 0.25)	1.2861	1.2013	1.2043
(0.5, 0.5, 0.5)	1.47	1.4381	1.4371
(0.75, 0.75, 0.75)	1.6955	1.713	1.7055
(1, 1, 1)	1.9622	2.0361	2.0318

Table 2 includes the different values of gradient coefficients (β) varying from 0 to 1 with the increment of 0.25. With the variation of β, normalized stress intensity factor also varies in increasing order. From the table, it is clearly observed that the results obtained from the partition of unity approach based on XFEM method in the present study are in very good agreement with those of Mohammadi [2008] and Guo and Noda [2007].

Table 3 shows the validation study of present first and second order perturbation technique (FOPT, SOPT) and independent Monte-Carlo simulation (MCS) by varying individual uncorrelated random system parameter $\{b4 = 0.05$ to $0.20\}$ on the normalized mean and COV of MMSIF for center cracked FGM plate subjected to uniaxial tensile, shear, combined tensile and shear stress for $\beta = 1.0$, $\theta = 0$, $a = 0.2$. The numerical results of the stochastic analysis of FGMs plate with single center crack subjected to different mechanical loadings along considered in this study are not available in the literature to the best of authors' knowledge. Therefore, to verify and validate the results of the present stochastic XFEM algorithm, results of moralized mean and COV MMSIF obtained through FOPT and SOPT are

Table 3. Comparison of normalized mean and COV of MMSIF using FOPT, SOPT and MCS $\{b_i(i = 4) = 0.05 - 0.20\}$.

COC	K_1			K_{II}		
	FOPT	SOPT	MCS	FOPT	SOPT	MCS
0.05	0.0590 (2.2144)	0.0580 (2.2327)	0.0575 (2.2214)	0.2747 (0.0305)	0.2733 (0.0305)	0.2742 (0.030143)
0.10	0.1320 (2.1556)	0.1220 (2.3326)	0.1251 (2.251)	0.6600 (0.0260)	0.6441 (0.0267)	0.6578 (0.0264)
0.15	0.1935 (2.1540)	0.1652 (2.5232)	0.1727 (2.342)	1.2019 (0.0222)	1.1252 (0.0237)	1.1701 (0.0229)
0.20	0.2810 (2.0988)	0.2094 (2.8161)	0.2481 (2.632)	1.9772 (0.0185)	1.7202 (0.0213)	1.8721 (0.01981)
0.25	0.3554 (2.1003)	0.2324 (3.2129)	0.2817 (2.875)	3.0918 (0.0154)	2.3895 (0.0199)	2.8112 (0.01721)
0.30	0.4623 (2.0484)	0.2507 (3.7783)	0.3253 (3.091)	4.7361 (0.0125)	3.0724 (0.0193)	3.4557 (0.0171)

compared with sampling-based MCS solutions. In MCS method, number of sample points required to perform the sample-based analysis is given; so 3500 number of sample points are utilized for satisfactory convergence of result. It is important to note that the MCS method utilizes higher computational cost when compared with perturbation technique and this is the reason behind use of perturbation technique in wide range of stochastic problems.

Table 4 shows the effect of individual random system parameter $\{b_i\ (i = 1, 2, \ldots, 9) = 0.10\}$ on the normalized mean and COV of MMSIF of central crack FGM plate in terms of K_{I} and K_{II} for $a = 0.2$, $\theta = 20$ $(\alpha, \beta, \gamma) = 0.80$ with the variation in loading. Among the given different random variables, random change in crack length and crack angle is most dominant when compared with other random variables. Hence, it is concluded that proper measurement and strict control of these random variables are highly important for reliability and safety point of view. However, randomness in material parameters is equally important when compared with fracture parameters.

Table 5 shows the effect of crack length with mechanical loadings on the normalized mean and COV $\{b_i\ (i = 4) = 0.10\}$ of MMSIF of FGM plate for $\theta = 15$ $(\alpha, \beta, \gamma) = 0.75$. For the same loading, with the increase of crack length, the mean and corresponding COV of MMSIF increase in general. It is concluded that crack length is one of the most sensitive parameters for providing safety and reliability of the center cracked plate. Accurate evaluation of crack length with minimum size

Table 4. Effect of individual random variables on the normalized mean and COV of K_{I} and K_{II} of central cracked FGMs plate subjected to uniaxial tensile, shear and combined loadings.

RV	SIF	Tensile		Shear		Combined	
		Mean	COV	Mean	COV	Mean	COV
E_{11}	K_{I}	1.7762	0.0001	0.4742	0.0011	1.2544	0.0004
	K_{II}	0.5933	0.0005	2.4967	0.0013	3.0899	0.0011
E_{22}	K_{I}	1.9735	0.0003	0.5269	0.0034	1.3938	0.0012
	K_{II}	0.6592	0.0007	2.7741	0.0019	3.4333	0.0016
υ_{12}	K_{I}	1.7779	0.0012	0.4670	0.0126	1.2641	0.0067
	K_{II}	0.5929	0.0001	2.5036	0.0041	3.0965	0.0033
G_{12}	K_{I}	1.7751	0.0004	0.4707	0.0048	1.2577	0.0017
	K_{II}	0.5924	0.0009	2.4860	0.0027	3.0784	0.0023
a	K_{I}	1.7257	0.0900	0.5463	0.1383	1.1443	0.1880
	K_{II}	0.5916	0.0686	2.4368	0.0788	3.0284	0.0768
θ	K_{I}	1.7123	0.0680	0.6853	0.0741	0.9865	0.8798
	K_{II}	0.6461	0.2958	2.3349	0.1028	2.9810	0.0164
α	K_{I}	1.7361	0.0001	0.4620	0.0011	1.2280	0.0004
	K_{II}	0.5796	0.0002	2.4364	0.0006	3.0160	0.0005
β	K_{I}	1.7361	0.0001	0.4620	0.0011	1.2280	0.0004
	K_{II}	0.5796	0.0002	2.4364	0.0006	3.0160	0.0005
γ	K_{I}	1.7361	0.0001	0.4620	0.0011	1.2280	0.0004
	K_{II}	0.5796	0.0002	2.4364	0.0006	3.0160	0.0005

Table 5. Effect of crack length on the normalized mean and COV of K_{I} and K_{II} of central cracked FGMs plate subjected to uniaxial tensile, shear and combined loadings.

Crack length (a)	SIF	Tensile		Shear		Combined	
		Mean	COV	Mean	COV	Mean	COV
0.1	K_{I}	1.4464	0.1933	1.0738	0.3399	0.3681	0.3872
	K_{II}	0.5726	0.3476	1.9749	0.2419	2.5475	0.1524
0.15	K_{I}	1.5192	0.1917	0.9277	0.2045	0.5759	0.2812
	K_{II}	0.5939	0.3306	2.1046	0.2108	2.6985	0.1273
0.2	K_{I}	1.6238	0.1990	0.7526	0.1921	0.8350	0.2159
	K_{II}	0.6247	0.3071	2.2228	0.1910	2.8475	0.1137
0.25	K_{I}	1.7670	0.1984	0.5833	0.3875	1.1159	0.1736
	K_{II}	0.6545	0.2808	2.3777	0.1765	3.0322	0.1093

is one way that the reliability of cracked structures can be increased. The COV of MMSIF is highest for combined loading, whereas mean is highest for tensile loading. Hence, proper attention of tensile loading is required for safety purpose of central cracked FGM plate.

Table 6 shows the effect of crack angle on the normalized mean and COV ($b_i\{i = 4\} = 0.10$) of K_{I} and K_{II} of edge cracked FGM plate subjected to uniaxial tensile stress and value of crack length maintained as $a = 0.2$ (α, β, γ) $= 0.65$. With the increase of crack angle, the mean of first mode SIF decreases while second mode SIF increases. The mean of first mode SIF is highest for tensile loading and lowest for shear loading. It is concluded that the cracked plate is safer and more reliable when crack angle is assumed as maximum as possible keeping the crack tip at center. It is concluded that crack angle is one of the very important parameters for safety and reliability of the plate.

Table 7 shows the effect of eccentricity (that is, the crack is 0.2 units above and below the central position of the plate) of crack length on the normalized mean and COV $\{b_i\ (i = 4) = 0.10\}$ of MMSIF of FGM plate for $\theta = 0$, $a = 0.2$, (α, β, γ) $= 0.45$. Whenever crack is below the center part of the plate, mean MMSIF

Table 6. Effect of crack angle on the normalized mean and COV of MMSIF ($b_i = \{i = 4\} = 0.1$) of K_{I} and K_{II} of center cracked FGM plate subjected to uniaxial tensile stress.

Crack angle (θ)	SIF	Tensile		Shear		Combined	
		Mean	COV	Mean	COV	Mean	COV
10	K_{I}	1.6437	0.1874	0.3029	2.7149	1.3109	1.2016
	K_{II}	0.4998	0.5482	2.3175	0.1580	2.8173	0.0327
25	K_{I}	1.3307	0.3030	1.3560	0.5824	1.3560	0.5824
	K_{II}	0.7261	0.1323	1.4619	0.5767	1.4619	0.5767
35	K_{I}	1.0501	0.3956	1.7475	0.1967	1.7475	0.1967
	K_{II}	0.8051	0.0057	0.6114	1.5509	0.6114	1.5509

Table 7. Effect of eccentricity on the normalized mean and COV ($b_i\{i=4\}=0.1$) of K_{I} and K_{II} of edge cracked FGMs plate subjected to uniaxial tensile stress.

e_y	SIF	Tensile		Shear		Combined	
		Mean	COV	Mean	COV	Mean	COV
0.2	K_{I}	1.8207	0.0004	0.5423	0.0801	2.2343	0.1188
	K_{II}	0.0690	0.0163	2.3279	0.0991	2.2843	0.0994
0.0	K_{I}	1.5688	0.1228	0.4502	2.7362	2.0045	0.7158
	K_{II}	0.2379	1.3928	2.2581	0.0863	2.4961	0.0724
−0.2	K_{I}	1.5043	0.0923	1.3164	0.2200	2.8206	0.1519
	K_{II}	0.0261	0.8619	2.2992	0.0974	2.3253	0.1060

is lowest while it is maximum above the center part of plate in case of combined loading. This is because maximum stress concentration occurs near or around the edge region of plate in tensile loading and in that case crack is below the center part.

Table 8. Effect of crack length and modulus ratios on the normalized mean and COV ($b_i\ \{i=4\}=0.1$) of K_{I} and K_{II} of edge cracked FGMs plate subjected to uniaxial tensile stress, $\theta=15$, $a=0.2$.

α,β,γ	SIF	Tensile		Shear		Combined	
		Mean	COV	Mean	COV	Mean	COV
0.1	K_{I}	1.1379	0.2628	0.5107	0.2727	0.6041	1.9267
	K_{II}	0.4379	0.3766	1.5135	0.2720	1.9515	0.1264
0.2	K_{I}	1.1982	0.2604	0.5407	0.2618	0.6328	1.9311
	K_{II}	0.4612	0.3765	1.6028	0.2710	2.0640	0.1263
0.5	K_{I}	1.4064	0.2541	0.6443	0.2314	0.7317	1.9438
	K_{II}	0.5413	0.3760	1.9080	0.2690	2.4493	0.1265

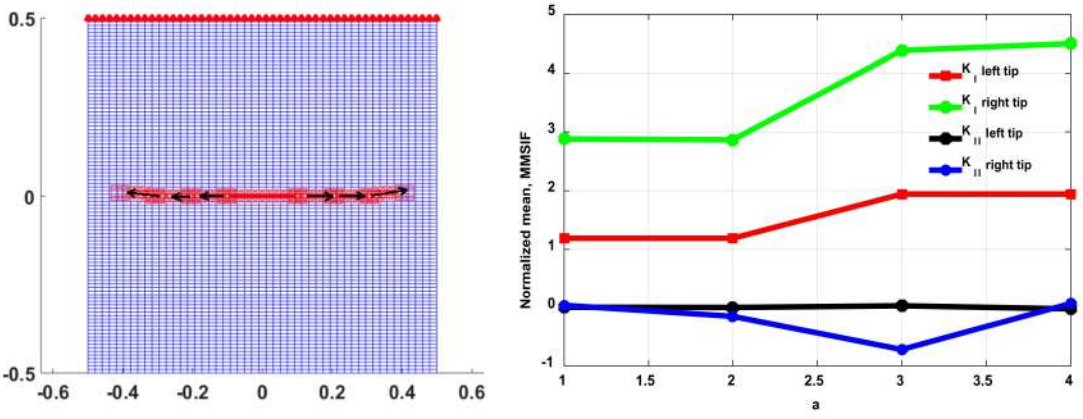

(a) Crack growth under tensile loading (b) MMSIF under tensile loading

Fig. 3. Effect of crack growth and number of steps on MMSIF subjected to (a) tensile loading, (c) shear loading, (e) combined loading, and corresponding MMSIF because of (b) tensile loading, (d) shear loading and (f) combined loading, respectively.

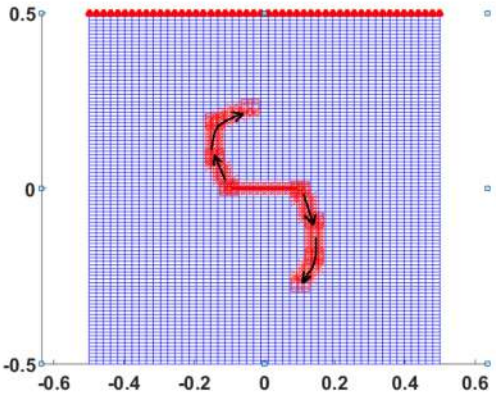

(c) Crack growth under shear Loading

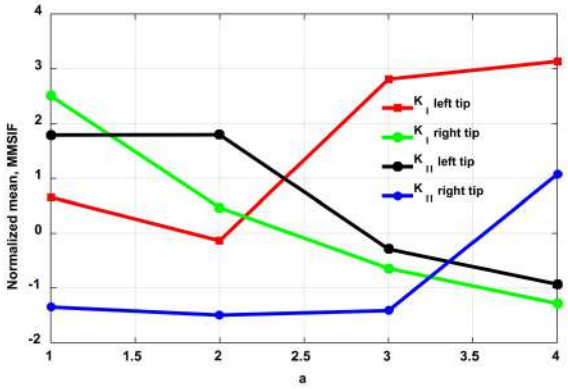

(d) MMSIF under shear Loading

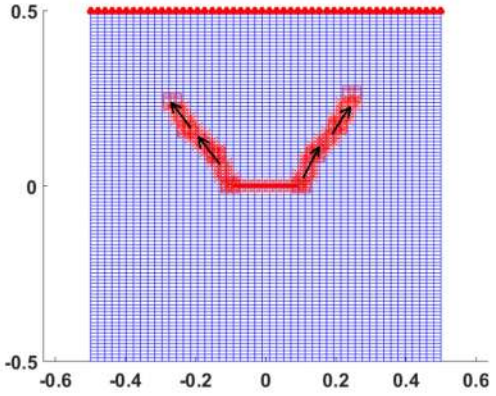

(e) Crack growth under combined Loading

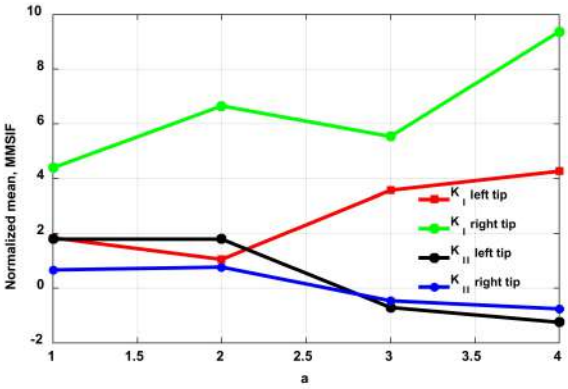

(f) MMSIF under combined Loading

Fig. 3. (*Continued*)

Table 8 includes the different values of gradient coefficients (α, β, γ) varying from 0.1 to 0.5. The observation shows that with the variation of gradient coefficients, normalized stress intensity factor also varies in increasing order.

Figure 3 shows the path followed by central crack subjected to tensile, shear and combined loadings with initial crack length ($a = 0.1$) and crack angle ($\theta = 0$) with crack propagation increment step being 0.1 keeping number of steps as 4. The obtained crack propagating path is almost parallel to crack and normalized first mode SIF increases while second mode SIF shows very little change when the plate is subjected to tensile loading. Crack path moving upward of the plate is subjected to shear and combined loading.

4. Conclusions

The stochastic XFEM combined with SOPT and MCS is used to evaluate the mean and COV of normalized mixed (KI and KII) mode SIF of single central crack FGM

plate subjected to uniaxial tensile, shear and combined loadings. The following conclusions can be noted from the limited study.

The mixed mode SIF of central crack FGM plate is most sensitive to the random change in the crack length, crack orientation, and elastic moduli of material. For safety factor of crack rectangular plate, these random system properties should be properly taken care; otherwise predicted response may be differing from actual response and resultant crack plate may be unsafe. It is interesting to note that effect of shear and combined loading is very dominant for mean of mixed mode SIF when compared with tensile loading. Hence, if small amount of these types of loadings is applied on the structure, there will be maximum chances of failure and fracture. However, it is surprising that small random change in system parameters, especially crack length and crack angle, makes the COV of cracked plate under tensile loading most dominant. It may be due to variation of crack parameters along axial direction.

For reliability and safety of cracked FGMs plate, lower crack length and higher crack angle above from center with higher modulus ratio are required. The position of crack at the center is most sensitive; hence, strict control of crack at the center is highly recommended. It is also very interesting that after changing the position of crack from center, sensitivity of crack decreases hence proper control of central crack is more important. Among the given different loading conditions, crack propagates parallel toward axial direction, while for shear and combined loadings it propagates toward downward and upward with axial direction, respectively. So from the study, better crack growth prevention can be possible.

References

Asadpoure, A., Mohammadi, S. and Vafai, A. [2006] "Crack analysis in orthotropic media using the extended finite element method," *Thin Walled Struct.* **44**(9), 1031–1038.

Asadpoure, A. and Mohammad, S. [2007] "Developing new enrichment functions for crack simulation in orthotropic media by the extended finite element method," *Int. J. Numer. Meth. Eng.* **69**, 2150–2172.

Belytschko, T. and Black, T. [1999] "Elastic crack growth in finite elements with minimal remeshing," *Int. J. Numer. Meth. Eng.* **45**(5), 601–620.

Besterfield, G. H., Liu, W. K., Lawrence, M. A. and Belytschko, T. [1991] "Fatigue crack growth reliability by probabilistic finite elements," *Comput. Meth. Appl. Mech. Eng.* **86**, 297–320.

Chakraborty, A. and Rahman, S. [2008] "Stochastic multiscale models for fracture analysis of functionally graded material," *Eng. Fract. Mech.* **75**(8), 2062–2086.

Chakraborty, A. and Rahman, S. [2009] "A parametric study on probabilistic fracture of functionally graded composites by a concurrent multiscale method," *Probab. Eng. Mech.* **24**(3), 438–451.

Chen, G. S., Rahman, S. and Park, Y. H. [2001] "Shape sensitivity and reliability analyses of linear-elastic cracked structures," *Int. J. Fract.* **112**(3), 223–246.

Evangelatos, G. I. and Spanos, P. D. [2011] "A collocation approach for spatial discretization of stochastic peridynamic modeling of fracture," *J. Mech. Mater. Struct.* **6**(7–8), 1171–1195.

Fleming, M., Chus, Y. A., Morant, B. and Belytschko, T. [1997] "Enriched element-free Galerkin methods for crack tip fields," *Int. J. Numer. Meth. Eng.* **40**, 1483–1504.

Guo, L. C. and Noda, N. [2007] "Modeling method for a crack problem of functionally graded materials with arbitrary properties — Piecewise-exponential model," *Int. J. Solids Struct.* **44**, 6768–6790.

Guo, L. C. and Noda, N. [2008] "Dynamic investigation of a functionally graded layered structure with a crack crossing the interface," *Int. J. Solids Struct.* **45**, 336–357.

Hadlar, A. and Mahadavan, S. [2000] *Probability Reliability and Statistical Methods in Engineering Design* (John Wiley & Sons Inc., New York).

Hadlar, M. H. and Sollero, P. [1998] "Crack growth analysis in homogeneous orthotropic laminates," *Compos. Sci. Tech.* **58**, 1697–1703.

Jamia, N., Borgi, S. E. I., Fernandes, R. and Vegamoor, V. [2016] "Analysis of an arbitrarily oriented crack in a functionally graded plane using a non-local approach," *Theoret. Appl. Fract. Mech.* **85**, 387–397.

Kaminski, M. M. [2002] *Computational Mechanics of Composite Materials*: *Sensitivity, Randomness and Multiscale Behaviour* (Springer-Verlag, London).

Khatri, K. and Lal, A. [2017] "Stochastic XFEM fracture and crack propagation behavior of an isotropic plate with hole emanating radial crack subjected to various in-plane loadings," *Mech. Adv. Mat. Struct.* **25**, 732–755.

Khatri, K. and Lal, A. [2018] "Stochastic FEM based fracture behavior and crack growth analysis of a plate with hole emanating crack under biaxial loading," *Theor. Appl. Fract. Mech.* **96**, 1–22.

Kleiber, M. and Hien, T. D. [1992] *The Stochastic Finite Element Method* (Wiley, New York, Chichester).

Lal, A. and Kapania, R. K. [2013] "Stochastic stress intensity factor response of single edge notched laminated composite plate," *54th AIAA/ASME/ASCE/AHS/ASC Structures, Structural Dynamics and Materials Conference*, Boston, Massachusetts, p. 1615.

Lal, A., Mulani, B. and Kapania, R. K. [2017] "Stochastic fracture response and crack growth analysis of laminated composite edge crack beams using extended finite element method," *Int. J. Appl. Mech.* **9**, 1–33.

Lal, A., Mulani, B. and Kapania, R. K. [2018] "Stochastic critical stress intensity factor response of single edge notched laminated composite plate using displacement correlation method," *Mech. Adv. Mater. Struct.*, doi:10.1080/15376494.2018.1506067.

Lal, A. and Palekar, S. P. [2016] "Probabilistic fracture investigation of symmetric angle ply laminated composite plates using displacement correlation method," *Curved Layer Struct.* **3**(1), 47–62.

Lal, A. and Palekar, S. P. [2017] "Stochastic fracture analysis of laminated composite plate with arbitrary cracks using X-FEM," *Int. J. Mech. Mater. Des.* **13**, 195–22.

Lal, A., Palekar, S. P., Mulani, B. and Kapania, R. K. [2017] "Stochastic extended finite element implementation for fracture analysis of laminated composite plate with a central crack," *Aero. Sci. Technol.* **60**, 131–151.

Lang, C., Dostan, A. and Maute, K. [2013] "Extended stochastic FEM for diffusion problems with uncertain material interfaces," *Comput. Mech.* **51**, 1031–1049.

Lin, Y. K. and Yang, J. N. [1983] "On statistical moments of fatigue crack propagation," *Eng. Fract. Mech.* **18**(2), 243–256.

Liu, W. K., Chen, Y. and Belytschko, T. [1996] "Three reliability methods for fatigue crack growth," *Eng. Fract. Mech.* **53**(5), 733–752.

Mohammadi, S. [2008] *Extended Finite Element Method for Fracture Analysis of Structures* (Blackwell, Oxford), 10.1002/9780470697795, Chapter 7.

Nouy, A. and Clément, A. [2010] "Extended stochastic finite element method for the numerical simulation of heterogeneous materials with random material interfaces," *Int. J. Numer. Methods Eng.* **83**, 1312–1344.

Nouy, A., Clément, A., Schoefs, F. and Moës, N. [2008] "An extended stochastic finite element method for solving stochastic partial differential equations on random domains," *Comput. Meth. Appl. Mech. Eng.* **197**, 4663–4682.

Nouy, A., Schoefs, F. and Moës, N. [2007] "X-SFEM a computational technique based on X-FEM to deal with random shapes," *Eur. J. Comput. Mech.* **16**, 277–293.

Rahman, S. [1995] "A stochastic model for elastic-plastic fracture analysis of circumferential through-wall-cracked pipes subject to bending," *Eng. Fract. Mech.* **52**(2), 265–88.

Rahman, S. [2000] "Probabilistic fracture mechanics: J-estimation and finite element methods," *Eng. Fract. Mech.* **68**, 107–125.

Rahman, S. [2006] "A dimensional decomposition method for stochastic fracture mechanics," *Eng. Fract. Mech.* **73**, 2093–2109.

Rahman, S. and Chen, G. [2005] "Continuum shape sensitivity and reliability analyses of nonlinear cracked structures," *Int. J. Fract.* **131**(2), 189–209.

Rahman, S. and Rao, B. N. [2001] "An element free Galerkin method for probabilistic mechanics and reliability," *Int. J. Solids Struct.* **38**, 9313–9330.

Rao, B. N. and Rahman, S. [2002] "Probabilistic fracture mechanics by Galerkin meshless methods — Part I: Rates of stress intensity factors," *Comput. Mech.* **28**, 351–364.

Reddy, R. M. and Rao, B. N. [2008] "Stochastic fracture mechanics by fractal finite element method," *Comput. Methods Appl. Mech. Eng.* **198**, 459–474.

Shrivastava, A. K. and Lal, A. [2013] "Determination of fracture parameters for multiple edge cracks of a finite plate," *J. Aircr.* **50**, 901–910.

Suresh, S. and Mortensen, A. [1998]. Fundamentals of functionally graded materials: Processing and thermomechanical behavior of graded metals and metal-ceramic composites (IOM Communications Ltd, London).

Tomar, V. and Zhou, M. [2005] "Deterministic and stochastic analyses of fracture processes in a brittle microstructure system," *Eng. Fract. Mech.* **72**, 1920–1941.

Xu, H. and Rahman, S. [2004] "A generalized dimension-reduction method for multidimensional integration in stochastic mechanics," *Int. J. Numer. Methods Eng.* **61**, 1992–2019.

Xu, H. and Rahman, S. [2005] "Decomposition methods for structural reliability analysis," *Probab. Eng. Mech.* **202**, 39–50.